Abstract

An analysis of microhardness and elastic modulus data for different lamellar systems in the light of both eutectoid copolymer and chain folded lamellar microphases is presented. A novel thermodynamically derived expression offering a fair description of hardness (stress required to plastically deform a crystal) of autonomous non-homogeneous microphases in terms of the average crystal thickness, including a defective surface boundary is developed. The present results characterize the mechanism of plastic deformation as primarily governed by the initial mosaic-block structure controlling the "solid state" mechanism underlined. The average dimensions of the remaining blocks after crystal destruction are, thus, related to the original block dimensions before plastic deformation. Within this context it is shown that the dissipated energy for crystal destruction increases very rapidly with the molar mass-function of crystalline material.

The elastic deformation of these lamellar systems at small strains is correlated to the rubber-like behaviour of the cluster-network. Finally, the role of the average thickness of the non-homogeneous microcrystallites is stressed as describing concurrently the elastic and plastics properties of the polymer allowing a quantitative description of the correlation found between microhardness and elastic modulus.

Key words: Semicrystalline polymers,
hardness
modulus
non-homogeneous micro-phase
structure

Introduction

The developing interest in polymeric materials with improved properties has led to many attempts to relate their macroscopic mechanical behaviour to that of the microscopic constituent phases. Several theoretical developments have been focused along this line to describe the mechanical behaviour of semicrystalline polymers using the two-phase concept /1-5/. In this picture the crystalline and "non-crystalline" regions are visualized as alternating stiff and compliant homogeneous micro-phases with well established intrinsic values. Application of this approach poses, nevertheless, certain difficulties when comparing different properties in the light of the detailed micro-structure of the model /6/.

The object of this paper is to offer from a thermodynamical and functional point of view a model approach for the microstructure of semicrystalline polymers relating to their elastic and plastic behaviour.Here, it is convenient to consider the system to be comprised of equivalent subunits of deformation with identical average intrinsic properties. The model of the cluster-network is based upon this concept. Accordingly, sufficiently large stacks of lamellar crystallites alternated by rubbery layers taken as such subunits, allows a comparably simple description of the small-strain modulus for semicrystalline polymers /7/.

According to this model the "macroscopic" definition of an autonomous phase, as a homogeneous part of the system having necessarily sharp interfaces, has to be adequately modified to the demands of a colloidical system like a semicrystalline polymer. It will be shown the possibility of operating with non-homogeneous "continuous" microphases possessing thermodynamically well defined intrinsic properties. The origin of the characteristics of these non-homogeneous microphases is related to the presence of defects in the stereoregularity of the chemical structure as well as in

restriction of conformational abilities on crystallization (chain folds or entanglements). From the lack of a thermodynamical compatibility of imperfections within the crystal lattice, it turns out that the defects are always rejected from the crystal core. The topological basic structure of these microphases thus demands the existence of non-autonomous defective interfaces /7-11/. The adequate phenomenological characterization of the latter is one of the crucial points of our considerations.

The capabilities of appropriate models are tested in the light of the mechanical properties, embracing both elastic and plastic deformation of polyethylene with different morphologies.

Basic Model

Polymers crystallize from the melt in the form of stacks of lamellar "crystals" alternated by non-crystalline (amorphous) layers. The lamellae are in turn, arranged within spherulites radially growing in all directions /20/. In recent papers /7,12,13/ we have proposed a model in which these lamellar stacks are considered to constitute "clusters". These clusters are assumed to represent the smallest functional elements which behave as "equivalent subunits of deformation" within a cluster network /7/. Within this context it is essential to properly understand the detailed organization within the clusters in order to adequately predict the macroscopic mechanical properties of the semicrystalline polymer.

It has been previously shown /7,8,22/ that a reasonable way of describing such polymer systems is through definition of thermodynamic "microphases". Within this context, one of the emerging problems is to describe the role played by the continuous interfaces

bridging the crystal cores and the rubbery amorphous layers. A general solution to this problem is offered in what follows.

Eutectoid Copolymer Lamellae /14/

The crystallization of linear copolymers consisting of randomly distributed eutectic comonomer units demands a controlled segregation of crystallizable CH_2-chain sequences (n_c) giving rise to a crystal stem thickness distribution. The latter is directly related to the distribution of the co-units along the chains:

$$(1) \qquad \Phi(y) = x_{nc}\, x_c^{y-1}$$

the molar fraction of the "non-crystallizable" units (nc-units) being defined through:

$$(2) \qquad x_{nc} = n_{nc}/(n_{nc}+n_c)$$

where n_c and n_{nc} are the molar numbers of the corresponding co-units.

According to this model the chain defects (for example short chain branches, unsaturations) are rejected from the coherently diffracting crystal core as "non-crystallizable units" (nc-units) into the longitudinal interfaces and "amorphous" regions. A defect-saturated extended CH_2-sequence mixed crystal, thus, arises as comprising c-sequences of different lengths with the maximum disparity in

sequence lengths given by:

$$\Delta y = A\, y + B \qquad (3)$$

where y is the average length of the c-sequences (in CH_2-units), and A and B are constants. A consequence of this model is that the average thickness of each longitudinal crystal interface Δy_B is described by

$$\Delta y_B = \Delta y/2 \qquad (4)$$

Figure (1) also depicts the average density, in accordance with the model, as a function of length. This picture is supported by SAXS investigations /15-18/. The crystal density ϱ_c is constant at the core and linearely diminishes along the increasingly distorted interface, reaching the minimum value, ϱ_a, for the amorphous layer within the interfaces (see fig. (1)).

Let us next define the size of the "non-homogeneous microphase", as an extended c-sequence mixed crystal (EMC), by the average length of the c-sequences, y, within the EMC. Most significant in this model is the fact that the internal properties of the non-homogeneous micro-phase (MP) are independent of its environment i.e. the microphase can be treated as a thermodynamically autonomous region. This is true in spite of the fact that the crystals are crosslinked by a fraction of tie-molecules, developing a three-dimensional network. The presence of tie-molecules does not severely impede the c-sequence segregation on crystallization so that flow of matter

(exchange of c-sequences!) is locally feasible /15/.

The molar mass fraction of the MP's, w_p, including the defective parts of each c-sequence, has been shown to be given by /14/:

$$w_p = x_c^{y-1} \left\{ (y-1)\, x_{hc} + x_c \right\} \tag{5}$$

y(T) is here associated to the lowest thermodynamically stable crystal at the temperature T (smallest possible thickness).

In contrast to the above definition, the "usual two-phase" molar mass fraction of crystallinity, w_c can be also derived from the model as:

$$w_c = \left(1 - A/3 \right) x_c^{y-1} \left\{ \left(y - 1 - y_k \right) x_{hc} + x_c \right\} \tag{6}$$

where

$$y_k = \left(B/3 - 1/2 \right) / \left(1 - A/3 \right) \tag{7}$$

Equation (6) sets out, of course, a systematically lower value for w_c as obtained from equation (5).

For the discussion of the results below it is convenient to define, as well, the following microstructural parameters:

a) Average thickness of crystal cores (coherently diffracting length)

(8) $$\langle y_{co} \rangle = x_c / x_{mc} + y - \Delta y/2$$

b) Average thickness of EMC s according to the usual two-phase model

(9) $$\langle y_c \rangle = (1 - A/3) (x_c / x_{mc} + y - y_k)$$

c) Average thickness in the assembly of non-homogeneous microphases summing up all c-sequences crystallized

(10) $$\langle y_p \rangle = x_c / x_{mc} + y$$

d) Average thickness of the amorphous interlayers representing, according to our model, homogeneous autonomous microphases as well. This parameter is derived from the cluster model as:

(11) $$\langle y_m \rangle = \langle y_p \rangle (1 - \omega_p) / \omega_p$$

Chain-Folded Lamellae

The densely stacking of lamellae a few hundred Angström thick, with large lateral widths, is featuring the microstructure of stereoregular homopolymers, particularly polyethylene, crystallized

from the undisturbed melt. Each lamella presents a uniform thickness, as evidenced by electron microscopy and Raman spectroscopy /19,20 /. Both the uniformity and the temperature dependence of the lamellar thickness are in support of the concept of chain folding at the lamellar surface /20/. Folding provides a means for ending up the growth of the crystal along the molecular direction, though a fraction of chains can be visualized as coming out from one lamella and entering the next one. These chains contribute to a threedimensional crystal network (see fig. (2)).

The treatment of alternating crystalline lamellae and disordered interlamellar layers as independent regions violates certain thermodynamic preconditions /8,9,10,21/. Thus, the present approach visualizes a chain-folded lamella as a non-homogeneous growth-constrained cooperative element possessing a limited autonomy due to the absence of a flow of matter. We further consider non-crystallizable defects, such as entanglements and molecular folds, as permanent defects to be located at the surface of the crystalline core. Hence, the average thickness of each lamella can be given by the average distances between the outer defects. The lamellae is seen according to this view, as a non-homogeneous microphase with a frozen in flow of matter which is otherwise analogue to the eutectoid copolymer MP. The degree of order of such a non-homogeneous microphase can be expressed as /8/:

$$(12) \quad w_i = (y_f - y_e)/y_f$$

where y_f is the average thickness of the chain folded lamella and $y_e/2$ is the corresponding average thickness of the distorted surface lamella (fig.(2)). Let us consider a lamella with sharp core-defective surface interfaces as having a surface free enthalpy 2

σ_e . The free enthalpy of the chain-folded lamellae is thus defined by:

$$(13) \qquad g_F = w_i g_c + (1-w_i) g_m + (2\sigma_e + g_{ex})/y_F$$

where g_c and g_m are respectively the free enthalpies per unit volume in the core and at the boundary. The excess term g_{ex} takes care for the average difference in enthalpy between the boundary and the melt.

The melting temperature of a "infinitely large" crystal is defined as

$$(14) \qquad T_m = \Delta h / \Delta s$$

where Δh and Δs are the usual molar-melting enthalpy and -melting entropy per chain unit respectively. The dependence upon temperature of Δh is given by /14/:

$$(15) \qquad \Delta h(T) = \Delta h(T_m) - \Delta C (T_m - T)$$

and ΔC is the molar temperature coefficient of the melting enthalpy.

From eqs. (12) and (13) and from the definition $g_{ex} = D/(1-w_i)$ one derives for the equilibrium degree of order $w_i(T)$ at constant y_f

$$(16) \qquad w_i = 1 - (D/y_F \Delta g)^{1/2} \; ; \quad \Delta g = \Delta h (1 - T/T_m)$$

where D is a parameter which characterizes the excess enthalpy of the permanent defects at the interface.

According to this model chain-folded crystallization is visualized as involving a local segregation of defects: As soon as on crystallization a crystal network is formed the number of permanent non-crystallizable defects increases during crystallization. A fraction of the defects is then attached directly to the surface of the chain-folded lamellae. The rest of them is located within the amorphous layers. Accordingly, the relative molar mass-fraction of folded chain lamellae w_f can be defined by /9/:

$$w_f = w_i^{n-1} \quad ; \quad n > 1 \tag{17}$$

Thus the total volume of crystallized material w_c can be expressed as:

$$w_c = w_i \, w_f = w_i^{n} \tag{18}$$

This equation is supported by thermodynamical reasons. Indeed, on the one hand, the defect concentration within chain folded lamellae is limited by stability considerations (defect-saturated microphase). On the other, the excess of permanent non-crystallizable defects is rejected from the chain folded lamellae, thus, contributing to the amorphous layer.

Finally, we postulate that the fraction of permanent defects within chain folded lamellae is related to the average density of

conformational defects or irregularities in the melt. The concentration of these defects should, on the other hand, be proportional to the ratio between the volume ($y^{3/2}$) occupied by the coiled chain and the excluded volume of a molecular chain itself (y). This ratio is proportional to $y^{1/2}$. If, on crystallization the total number of these conformational defects is preserved, then, the parameter, D, characterizing the defective interphase will be proportional to $y^{1/2}$. However, since crystals with extended stems of thickness $y < y_c$ having no other permanent defects as chain ends (the excess contribution of the chain ends is included in $2\sigma_e$), also appear, D will be consequently proportional to:

$$D = \alpha\left(y^{1/2} - y_c^{1/2}\right) \tag{19}$$

The latter equation underlies the fact that permanent non-crystallizable defects represent a relevant feature of chain folded crystallization whereby the value of y_c is dependent of the crystallization history / 20 /.

Small Strain Modulus of Cluster Networks

The elastic behavior of the cluster-network can be conveniently explained under the assumption that the stresses in the crystal lamellae and amorphous layers are equal. In contrast to usual two-phase model theories we shall use the autonomous subunits as essential elements for describing the elastic response of the semicrystalline system.

Figure (3) schematically illustrates clusters of lamellae consisting of mosaic blocks alternated by amorphous layers. The clusters are connected by means of tie-molecules to the neigbouring ones. For the

description of the macroscopic elastic properties it is sufficient to analyse the microstructure of one representative cluster using the average values of the structure parameters. The elastic modulus of such a cluster, E, has been shown to approximate to a series model /7/ of crystal lamellae as defined by the MP's, separated by amorphous layers:

$$\frac{1}{E} = \frac{w_p}{E_p} + \frac{1-w_p}{E_m} \tag{20}$$

where E_p is the quasi-isotropic, averaged modulus of the MP's embracing its defective boundaries. The modulus of the rubbery amorphous layers E_m can, on the other hand, be written as:

$$E_m = 3G_o T / \langle \gamma_m \rangle = \left(\frac{3G_o T}{\langle \gamma_p \rangle} \right) \frac{w_p}{1-w_p} \tag{21}$$

where G_o is a constant, and T the absolute temperature. According to this concept, each crystal is considered as a multifunctional crosslinked body, in which the number of linkages is equalling the number of chains emerging from the crystals. This assumption justifies the $\langle \gamma_p \rangle^{-1}$ dependence of E_m.

Hardness relating to Microstructure

Microidentation hardness is measured by quasi-static penetration of the specimen surface with a standard indenter at a given force and temperature /22/. A convenient measure of hardness is obtained by dividing the peak-contact load, p, by the projected area of

impression A

(22) $$H = k^* p / A = k p \delta^{-2}$$

where k^* is a constant, $k^* = 18.191\ 10^3$, and δ is the penetration depth of the indenter within the surface for a Vickers pyramid $\delta = \sqrt{A}/7$ /23/, ($[H] = MN\ m^{-2}$; $[p] = 9.81\ 60^{-3} N$, $[\delta] = 10^{-6} m$).

The hardness, so defined, can be considered as an indicator of irreversible plastic deformation of a small volume element (typically $V_1 \sim 10^{+11}$ nm ^{3}). The rest of the material acts as a constraint.

The hardness of a semicrystalline polymer can be visualized as that of a material consisting of separate distinct hard and compliant elements /24/. On the basis of the above model we suggest:

(23) $$H = w_p H_p + (1-w_p) H_m$$

where H_p and H_m are the intrinsic hardness values of the MP's and the amorphous layers respectively.

In a previous study we have investigated the zone of material destruction under the indenter /24/ involving a volume element V_{cd}.

Since $H_p \gg H_m$ it turns out that the heat dissipated by plastically deformed crystallites is given by

(24) $$\Delta\phi_{cd} = \Delta\phi / V_{cd}$$

where the volume V_{cd} can be written as

(25) $$V_{cd} = \alpha A \delta$$

The mechanical work which is performed must be equal to:

(26) $$W = p\,\delta = \Delta\phi$$

Hence, by using equations (24), (25) and (26) we are led straightforwardly to the relationship:

(27) $$H_p = H_o\,\Delta\phi_{cd} \quad ; \quad H_o = K/\alpha \quad (\ p = \text{const}\ )$$

Since indentation involves yielding, it seems plausible that a substantial destruction of crystallites would take place /24/. Therefore, it is interesting to express V_{cd} in terms of the micro-structural elements left after such a severe deformation. Let us assume that the destruction of crystallites is "heterogeneous" and involves the generation of a more or less dense system of shear-planes, wherein the energy is grossly dissipated (see fig. (4)). By assimilation of the original MP to cubes, the relative fraction of the "shear planes" is straightforwardly obtained to a first approximation from the ratio:

(28) $$\text{surface}/_{\text{volume}} \approx \langle y_p \rangle^{-1}$$

Hence, we can approximate V_{cd} to

(29) $$V_{cd} = V_o \left(1 + b_1 \langle y_p \rangle^{-1} \right)$$

Thus one can rewrite equation (17) as:

(30) $$H_p = H_o \, \Delta\phi / V_{cd}$$

$$H_p = H_o \, \Delta\phi^* / \left(1 + b_1 \langle y_p \rangle^{-1} \right)$$

This expression is of major interest because it relates the "crystal hardness" of a material to the size $\langle y_p \rangle$ of the cooperative units building the mosaic block structure. It is worth noting that for $\langle y_p \rangle \rightarrow \infty$, H_p approaches to $H_o \, \Delta\phi^*$, which is the maximum value of dissipated energy by plastic deformation which can be reached (for PE: $H_o \, \Delta\phi^* \cong 170$ MN m^{-2} /24/).

From equation (30) one can, therefore, reasonably predict that H_p, as a measure for intrinsic plastic deformation, substantially decreases with decreasing size of the constituent PM's. The relevance of the phenomenological b_1-factor in equation (30) will be discussed further below in the light of experimental data for polyethylene with different morphologies.

Discussion

Hardness data for Different Lamellar Systems

Most interesting is the analysis of hardness values for different lamellar systems in the light of both, eutectoid copolymer- and chain-folded lamellae micro-phases. For this purpose we have selected a variety of hardness data from references /22-25/. Figure (5) illustrates the plot of H_p as a function of $\langle y_p \rangle^{-1}$ for a series of chain-folded- and short-chain branched polyethylenes and n-paraffins. The plot shows an excellent agreement with the calculated values according to equation (30) if one uses for b_1 a value of b_1 = 20 nm. This value of b_1 applies just for samples crystallized at atmospheric pressure /26/. We have shown, in fact, that b_1 is a decreasing function of crystallization pressure /26/. Thus, for PE samples crystallized, for instance, at a pressure of 150 MN/m^2 a fitting constant b_1 = 10 nm is required.

Equation (30) allows a direct description of the hardness of the MP's (autonomous non-homogeneous micro-phases) in terms of $\langle y_p \rangle$, average crystal thickness including the defective surface boundary. It is interesting to note that n-paraffins can equally well be described by means of equation (30) simply by using the chain-length parameter.

Let us next discuss the micromechanism of plastic deformation from the initial structure into its final state. Since the dissipated heat per unit volume V_o can be equated to

(31) $$\Delta\Phi^* = \Delta\Phi / V_o = p\delta / V_{cd}$$

we admit that plastic deformation of crystals mainly proceeds by a multitude of shearing planes. Therefore, on the basis of a cubic

schmelz entalpie

symmetry for the cross-section of the MP's we are led to

(32) $$\Delta\phi / \cancel{V_0} = (\Delta h / \cancel{V_0})(4a_0/l_p)$$

where a_o is the average lateral intermolecular distance within the crystals. The parameter l_p describes now the average lateral dimensions of final "crystal blocks" left, having in the average the invariant thickness $\langle y_p \rangle$. By combination of equation (31)

(33) $$l_p = \frac{4\Delta h}{\cancel{V_0}} \frac{V_{cd}}{\rho\delta} a_o$$

Furthermore, with equations (29) and (33) we arrive at:

(34) $$l_p = K(1 + b_1 \langle y_p \rangle^{-1}) a_o/\delta$$

This equation relates the average dimension of the newly created blocks l_p to the dimensions of the original mosaic blocks before plastic deformation (see fig.(4)). Table (1) collects the l_p-and $\langle y_p \rangle$ -values for a series of branched polyethylenes, together with the average values of the lateral coherent dimensions of the original system $\langle D_c \rangle$ and the ratio $n_a = \langle D_c \rangle / l_p$, which is proportional to the number of defects produced on plastic deformation.

These data indicate that the final dimension l_p is nearly independent from the initial mosaic length. In addition it is seen

that l_p corresponds to 4-5 intermolecular distances yielding elementary "crystal rods" constituted by 16 to 25 stems. The ratio n_a diminishes, however, notably with decreasing size of the original mosaic blocks. Figure (6) shows the linear correlation found between the reciprocal value of n_a the molar degree of crystallinity (eqs.(6) and (18)). These data further illustrate the fact that the maximum number of shearing planes increases progressively with crystallinity.

Thus, for a fully crystallized lamellar system with a thickness $\langle y_p \rangle$, the number of shearing planes tends to infinity despite having a constant final limiting size l_p. Conversly, for low crystallinities the original mosaic blocks are so small that they are nearly unmodified after plastic deformation. These results illuminate the view of plastic deformation of semicrystalline colloidal systems as exclusively governed by the primary mosaic-block structure regulating the intrinsic "solid state" deformation mechanism. It is also found that this mechanism is independent of the cluster-structure, thus, supporting the concept of non-homogeneous microphase as a cooperative structural unit with independent intrinsic properties.

Figure (7) illustrates the striking increase of dissipated energy with rising molar mass-fraction of crystalline material. The solid line has been computed according to (table (1))

$$(35) \qquad {}^{i}W_{diss}\, C^{*} = 4 \langle y_p \rangle l_p w_p$$

It is evident that the smallest crystals contribute with a negligible dissipated energy to the overall deformation energy in the total

system. This solid state deformation process increases, however, dramatically for very large MP's. This is so because w_c and $\langle y_p \rangle$ are strictly correlated according to tables (2) and (3).

Small-Strain Elastic Modulus

Contrary to the mechanism of plastic deformation discussed in the previous section, the elastic deformation at small strains is correlated to the reversible behavior of the cluster-network /7/. This is demonstrated in figure (8B) by the unique correlation obtained between E and w^c. The solid line has been computed with the aid of equations (6), (20) and (21). The parameters used are listed in table (2). The experimental data obtained for commercial branched polyethylenes /25/ fit very well indeed with the theoretical predictions suggesting a random distribution of branches along the chains for c-sequences larger than $y \gtrsim y_{MIN} = 27$ chain units.

Moreover, E and H are found to be correlated (see figure (8A) as calculated with the aid of the equations (6), (20), (21) (solid line in fig. (8A), table (2)).

Fig. (9) illustrates, likewise, the good correlation obtained between E and the molar mass fraction of MP's for a series of linear chain folded polyethylene samples having two different molecular weights (see table (3)) and various morphologies /22/. The data adjust very well to the predictions derived from the combined description of hardness and small-strain elasticity (see next section).

The data for branched polyethylenes /25/ are also included for comparison and seem to fit roughly the "master curve". However, for larger mass fractions w_p one detects a systematic discrepancy for

the branched materials yielding larger E-values than for folded-lamellar polyethylenes. This means that, at least in the case of EMC's, the elastic storage properties of the amorphous layers for branched PE are somewhat better than for folded-chain polyethylene.

The unique plot obtained in figure (9) shows the advantage of using the parameter w_p instead of the usual molar mass fraction of crystals, w_c, in analysing the elastic properties. Indeed a more complex picture arises when using w_c (see fig. (10)).

The Role of the Non-homogeneous Microphase Relating to the Elastic- and Plastic-Behavior

By inspection of eqs. (20), (21), (25) and (30) one immediately detects a parallel dependence of $E(w_p, \langle y_p \rangle)$ and $H(w_p, \langle y_p \rangle)$ justifying the theoretical prediction of a distinct correlation between both quantities E and H (see also fig. (8)). Such a correlation has been previously disputed by several authors /23,27,28/.

Fig. (11) illustrates the experimental relationship obtained between E and H /15,18/ for chain-folded and branched polyethylenes. The solid line Co in fig. (11) is straightforwardly derived from eqs. (5), (20), (21), (25) and (30) by using the parameters listed in table (2).

The solid line (F) was obtained by using eqs. (16),(17) and (25), (30) and adjusting the parameters n and y_f conveniently. The data are recorded in table (3). Fig. (12) shows the parallel relationship between n and y_f for the two linear polyethylenes with different

molecular weights. This result is somehow surprising in contrast to previous observations of polyethylene fractions and indicates the complexity of crystallization behavior probably influenced as well by the molecular weight distribution /8, 30-32/.

These results underline the dominant role of the average thickness of the non-homogeneous micro-crystallites, $\langle y_p \rangle$, in describing the plastic and the elastic properties of semicrystalline polymers: Thus, whereas the plastic properties are mainly governed by the intrinsic behavior of crystals regulated mainly by $\langle y_p \rangle$, the elastic response, on the other hand, is dictated by the cooperative effects of both microphases within the cluster-network. This difference is best illustrated by the different dependence of the overall hardness upon the modulus E (see curves F and Co in fig. (11)).Since micro-hardness is dominantly correlated to $\langle y_p \rangle$, the difference between F and Co admittedly arises from the more pronounced rubberelastic behavior of the amorphous layers in branched polyethylenes.

Concluding Remarks

In summary, the discussed results justify the correlation obtained between elastic modulus and microhardness for a series of polyethylene samples within the framework of the concept of autonomous microphases as constituent elements of clusters. The above picture demands that the "crystals" are built up by a well ordered core having a well differentiated defective surface-layer providing a continuous bridge to the amorphous region. In concept of equivalent units of deformation within a cluster-network allows, then, a quantitative description of the small-strain modulus while the hardness mainlky depends on the plastic deformation of the crystals as non-homogeneous solid microphases.

Acknowledgements

One of us (FJBC) is indebted to the University of Ulm for the tenure of a visiting professorship and to CAICYT, Spain for the support of the work.

Wir danken auch der Deutschen Forschungsgemeinschaft für Unterstützung.

References

1. Hill R (1963) J Mech Phys Solids, II: 357
2. Takayanagi M (1965) Proc Fourth Intern Cong Rheology Part I, p. 161, Inerscience Publ N.Y.
3. Halpin JC, Kardos JL (1972) J Appl Phys 43: 2235
4. Patel J, Philips PJ (1973)
5. Arridge RBC (1975) "Mechanics of Polymers", Clarendon Press, Oxford, p.97
6. Andrews EH (1974) Pure and Applied Chem, 39: 179
7. Kilian HG (1984) Coll & Polym Sci 262: 374
8. Holl B, Heise B, Kilian HG (1983) Coll & Polym Sci 261: 978
9. Baur H (1982) Coll & Polym Sci 260:370
10. Zachmann HG (1964) Fortschr. Hochpolymerforschung 3: 581
11. Kanig G (1982) Coll & Polym Sci 260: 356
12. Heise B, Kilian HG, Wulff W (1980) Progr Coll & Polym Sci 67: 143
13. Kilian HG, Pietralla M (1978) Polymer 19:664
14. Glenz W, Kilian HG, Klattenhoff D, Stracke Fr (1978) Polymer 18:685
15. Heise B, Kilian HG, Schmidt H (1981) Coll & Polym Sci 259:611
16. Hosemann R, Bagchi SN (1962) Direct Analysis of Diffraction by Matter North-Holland Amsterdam
17. Kilian HG, Wenig W (1974) J Macromol Sci B9:463
18. Meyer H, Kilian HG (1978) Progr Coll & Polym Sci 64:166
19. Duglosz J, Fraser GV, Grubb D, Keller A, Odell JA, Goggin PL (1977) Polymer 17:471
20. Wunderlich B (1973) Macromolecular Physics, Vol 1, Academic Press NY and London
21. Baur H (1978) Coll & Polym Sci 256: 833
22. Baltá-Calleja FJ (1984) Advances in Polym Sci "New Developments in the Characterization of Polymers in the Solid State" 67-68
23. Baltá-Calleja FJ (1976) Coll & Polym Sci 254: 258
24. Baltá-Calleja FJ, Martinez-Salazar J, Cackovic H, Loboda-Cackovic J (1981) J Mat Sci 16: 739
25. Martinez-Salazar J, Baltá-Calleja FJ (1983) J Mat Sci 18:1077
26. Baltá-Calleja FJ, Rueda DR, Garcia J, Wolf FP, Karl VH, J Mat Sci (in press)
27. Baer E, Maier R, Peterson N (1961) SPE J 17: 1203
28. Bowman J, Bevis M (1977) Coll & Polym Sci 255: 954

29. Kilian HG (1982) Coll & Polym Sci 260:374
30. Fatou JG, Mandelkern L (1964) J Phys Chem 69:417
31. Maxfield J, Mandelkern L (1977) Macromolecules 10:1141
32. Voigt-Martin IG, Fischer EW, Mandelkern L (1980) J Polym Sci 18:2347

table (1)

x_{nc}	$\langle y_p \rangle$ /nm		$\langle D_c \rangle$ /nm	w_p/mol%	w_c/mol%	lp/nm	n_a	$W_{diss}C^*$
0.0019	26.0		171	0.997	0.922	1.95	8.8	3957
0.007	27.0		148.5	0.979	0.849	1.78	8.3	2980
0.0176	12.0		109	0.908	0.708	1.95	5.6	1182
0.0263	10.8	86	98.5	0.829	0.605	2.30	4.3	1068
0.0304	10.0	80	80.5	0.789	0.56	1.60	5.0	674
0.0361	9.0	72	64.5	0.731	0.502	1.58	4.1	526
0.048	7.0	56	75.5	0.612	0.396	1.63	4.6	353
0.0534	5.8	46	98	0.561	0.355	2.12	4.6	452
0.069	5.0	40	50	0.425	0.254	1.57	3.2	180

table (2)

x_{nc}	w_o/%	w_c/%	$\langle y_p \rangle$/nm	H_p / MN m^{-3}	H / MN m^{-3}	E / MN m^{-2}
0.005	0.986	0.856	28.9	100	99	2107
0.01	0.956	0.77	16.1	76	73	1728
0.015	0.916	0.691	11.9	64	59	1208
0.02	0.868	0.618	9.7	57	49	784
0.025	0.816	0.552	8.4	51	42	507
0.03	0.761	0.493	7.6	48	36	338
0.04	0.649	0.389	6.5	43	28	167
0.05	0.542	0.306	5.9	40	22	93
0.06	0.445	0.238	5.5	38	17	57
0.07	0.361	0.184	5.2	36	13	37

$\Delta h(T_M)$ = 970 cal/mol unit

$2\ \sigma_e(T_M)$ = 2050 cal/mol unit

T_M = 415 K

H_m = 0.5 MN m^{-3}

H_c = $H_o\ (y_c^{1/2} - C)$

C = 10

H_o = 6.5 MN m^{-3}

A = 0.15

B = 46

T = 295 K

E_c = 2.2 10^3 MN m^{-2}

G_o = 2 MN m^{-2}

y = 29 Fraktile

table (3)

Molecular-weight: $2\ 10^6$

n [1]	y_f/nm	w_p/mol%	w_c/mol%	H_k / MN m^{-3}	H / MN m^{-3}	E / MN m^{-2}
1.3	400	0.955	0.818	113	108	1227
1.55	200	0.883	0.704	85	75	563
1.8	100	0.763	0.544	57	43	278
2	60	0.63	0.40	39	24	165

Molecular-weight: $1.5\ 10^5$

n [1]	y_f/nm	w_p/mol%	w_c/mol%	H_k / MN m^{-3}	H / MN m^{-3}	E / MN m^{-2}
1.7	400	0.95	0.884	113	108	1124
2.2	200	0.882	0.795	85	75	558
2.7	100	0.773	0.665	57	44	305
3.2	60	0.644	0.528	39	25	182

$H_c = H_o\ \Delta\phi^*\ /(1+b_1\ \langle y_p \rangle^{-1})$; $\quad \alpha = 5$

$(H_o\ \Delta\phi^*)_\infty = 170$ MN m^{-3} $\quad y_c = 300$ nm

other parameters are listed in table (2)

1) see equation (17)

Legend to Figures

Fig. 1: Model of an extended c-sequence mixed crystal illustrating the rejection of defects (nc units) from the coherently diffracting core (ϱ_c, ϱ_m density of in the crystal lattice and in the non-crystallized regions).

Fig. 2: Model of chain folded crystal having a crystallographic ordered core and a non-crystallizable interphase consisting of chain folds, loops and entanglements.

Fig. 3: The elastic behaviour of a semicrystalline polymer can be described in terms of the cluster-network model: Lamellar stacks (clusters) consisting of mosaic blocks alternated by amorphous layers are connected to neighbouring clusters by means of many tie molecules.

Fig. 4: Model of deformation of lamellae consisting of mosaic blocks beneath the stress-field of an indenter A heterogeneous destriction of crystals involving the generation of a system of shear planes is assumed.

Fig. 5: Microhardness of "crystals", $H_p \cong H/w_p$, against reciprocal average thickness of non-homogeneous microphase according to eq. (30). Data for PE crystallized at: $\Delta T \simeq 10°C$ (O); $\Delta T \geq 68°C$ (O) (24) and melt crystallized paraffins (+) (23).

Fig. 6: Correlation between reciprocal number of shearing planes $n_a = \langle D_c \rangle / lp$ after crystal destruction and the molar degree of crystallinity.

Fig. 7: Increase of dissipated energy during crystal destruction as a function of molar mass fraction of crystalline material.

Fig. 8: Correlation of elastic modulus E and microhardness, H (A) and modulus E and crystallinity w_c (B) as predicted from eqs. (6), (20) and (21) (solid lines). Experimental data for branched PE are taken from ref. 25.

Fig. 9: Correlation of modulus E and the molar fraction of MP's, w_p, from the theoretical predictions derived in table 3.
Data for linear chain folded PE samples with $M_w = 2 \times 10^6$ (O); $M_w = 1.5 \times 10^5$ (O) and branched materials (Δ) are from refs. 22 and 25.

Fig. 10: Plot of elastic modulus versus crystallinity for:
a) branched PE, and chain folded PE with: b) $M_w = 2x10^6$
and c) $M_w = 1.5x10^5$.

Fig. 11: Correlation of microhardness and plastic modulus. The solid lines were obtained using eqs. (16), (17) and (25), (30). The parameters used are given in table 3. The experimental data are taken from refs. 22 and 25.

Fig. 12: Plot n as a function of thickness of non-homogeneous micro-crystallites for two linear polyethylenes with differing molecular weight.

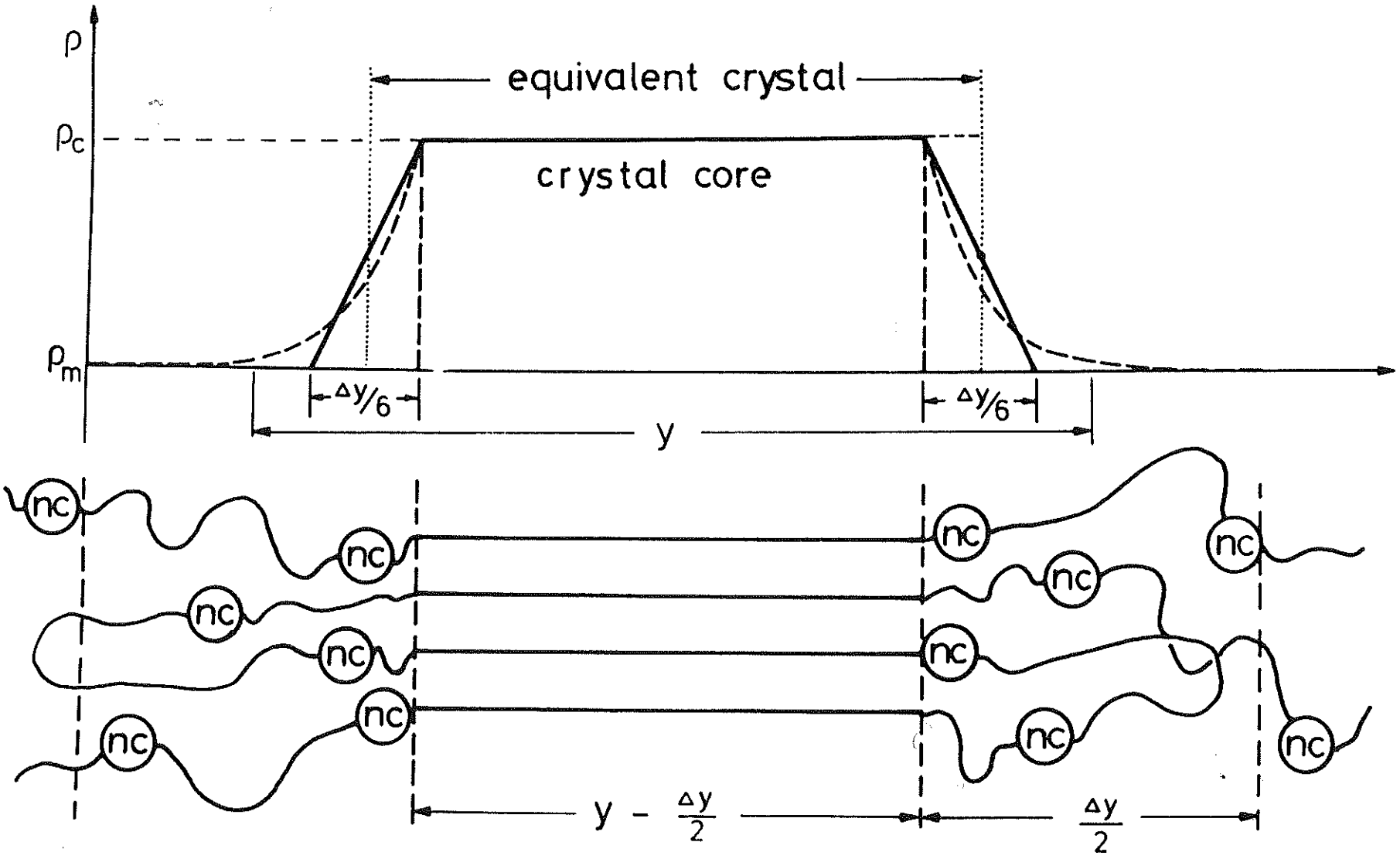

Fig. 1

Fig 2

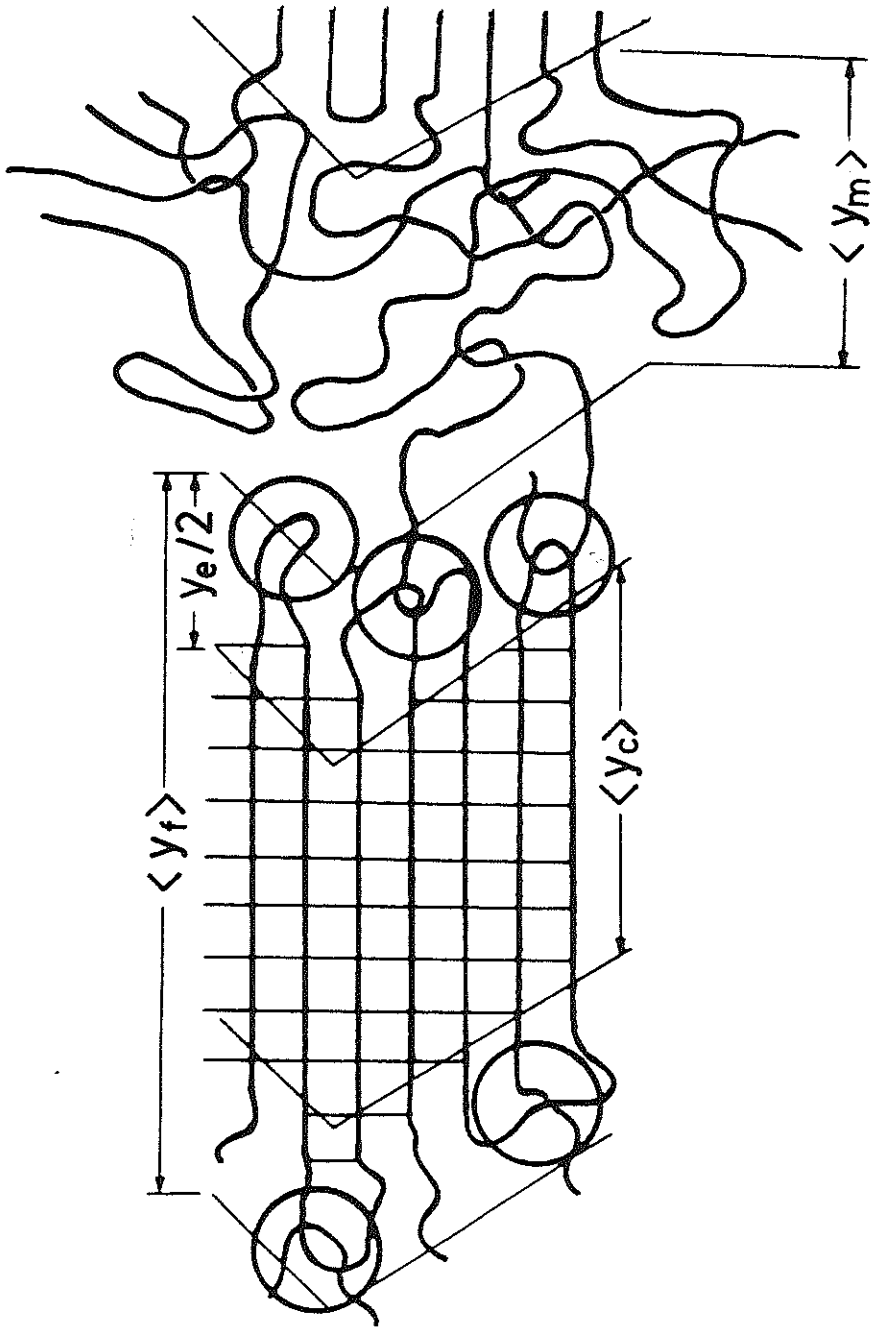

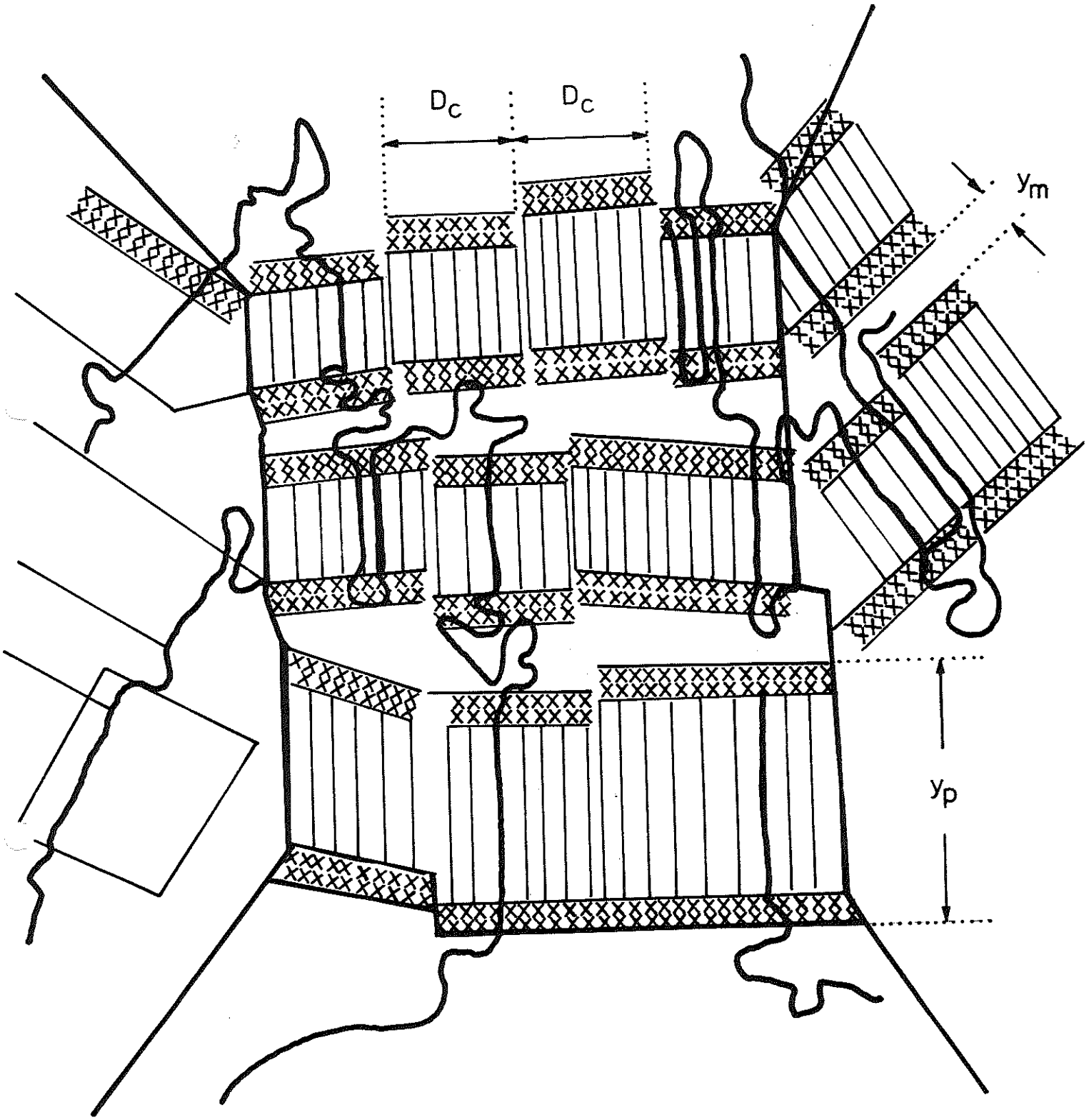
D_c
D_c
y_m
y_p

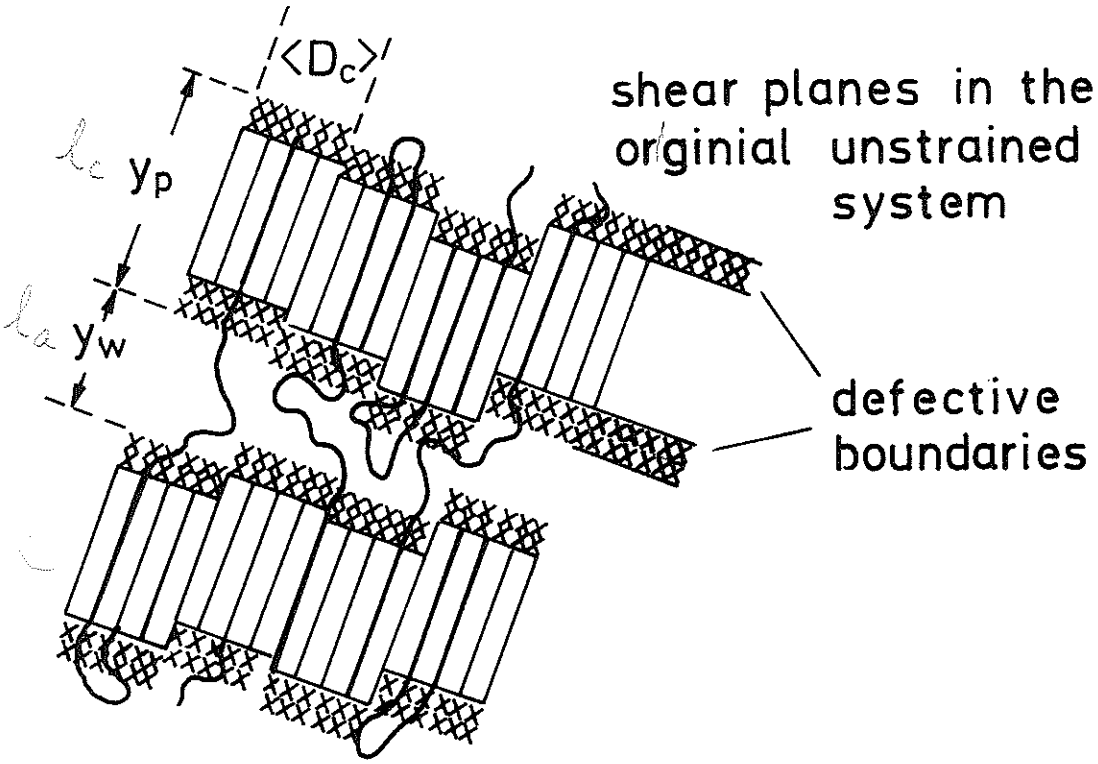

plastic deformation

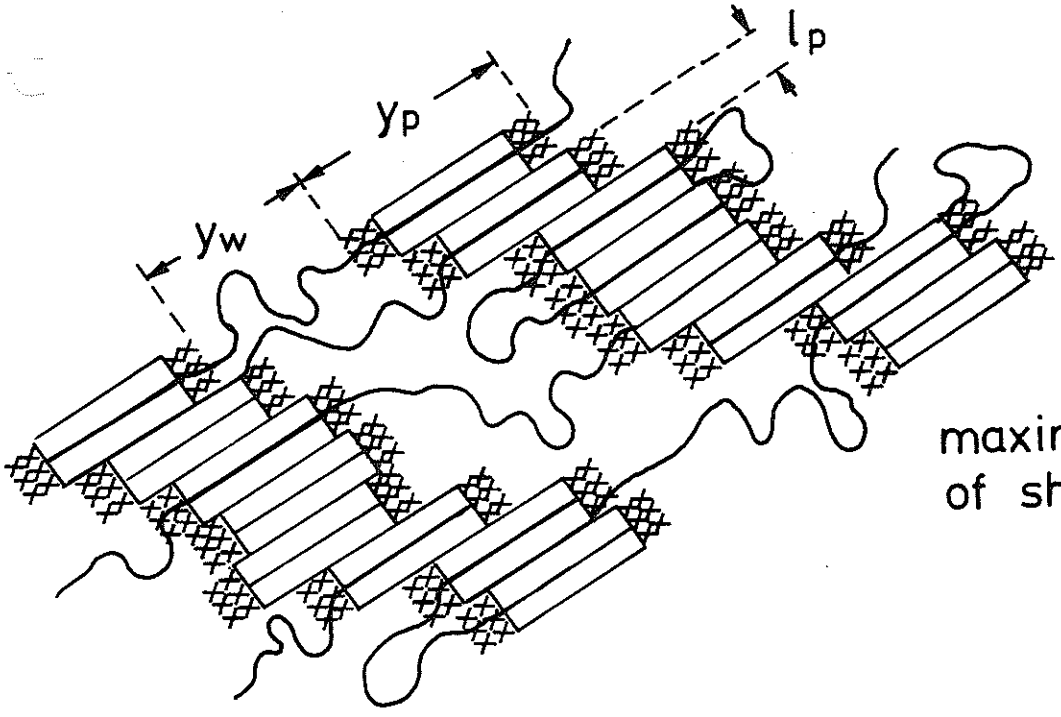

Fig. 5

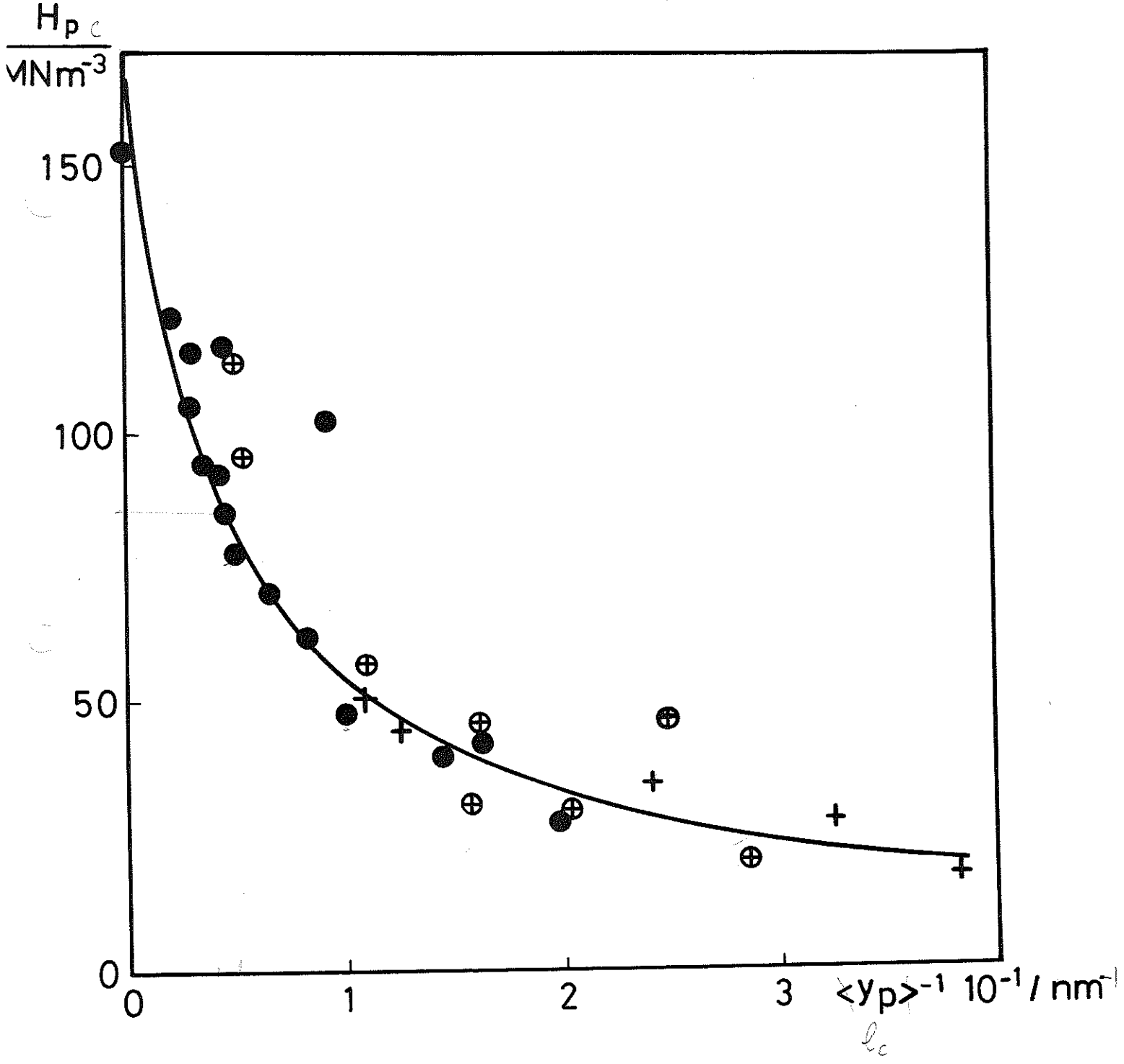

Fig. 6

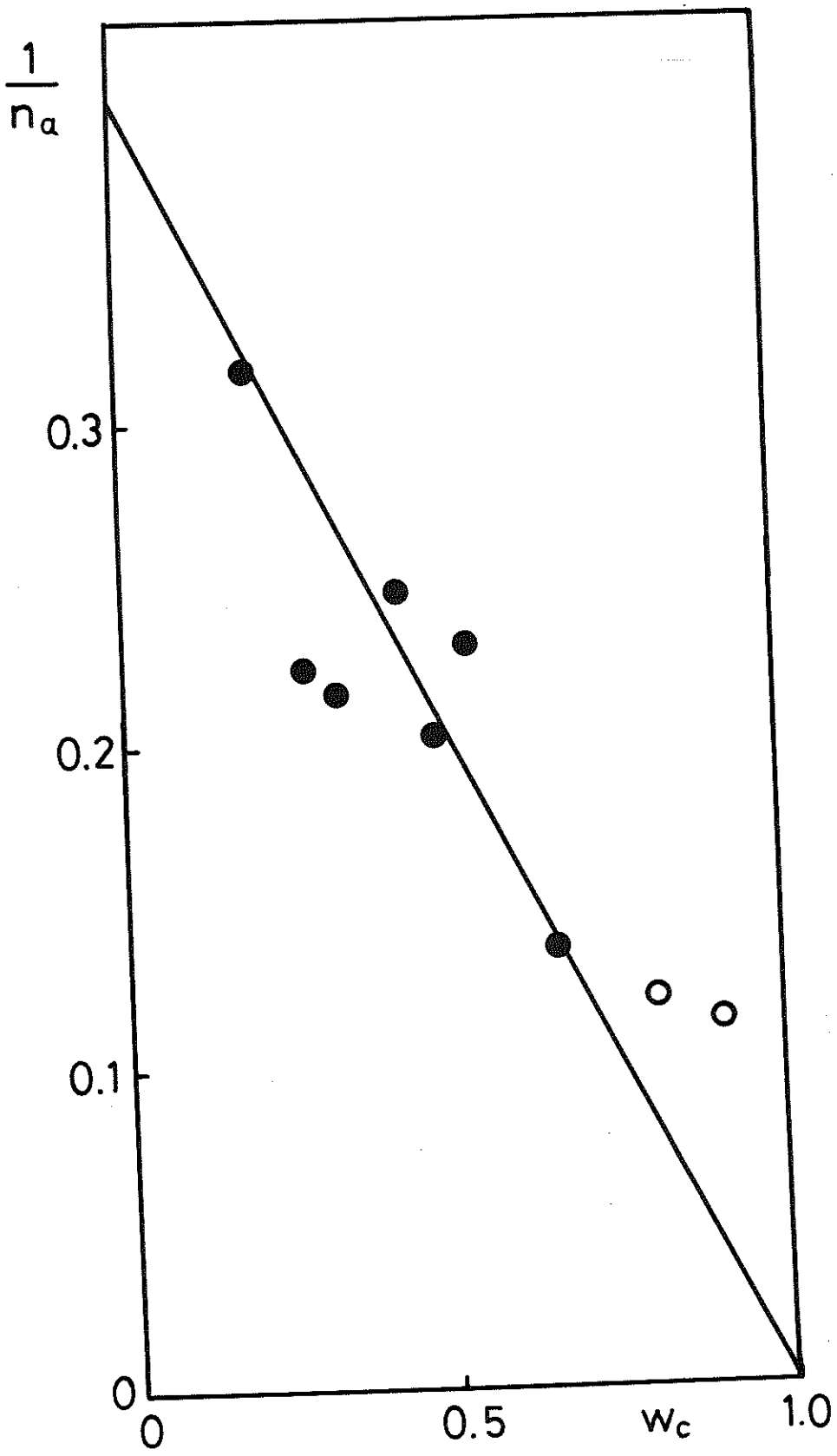

Fig. 7

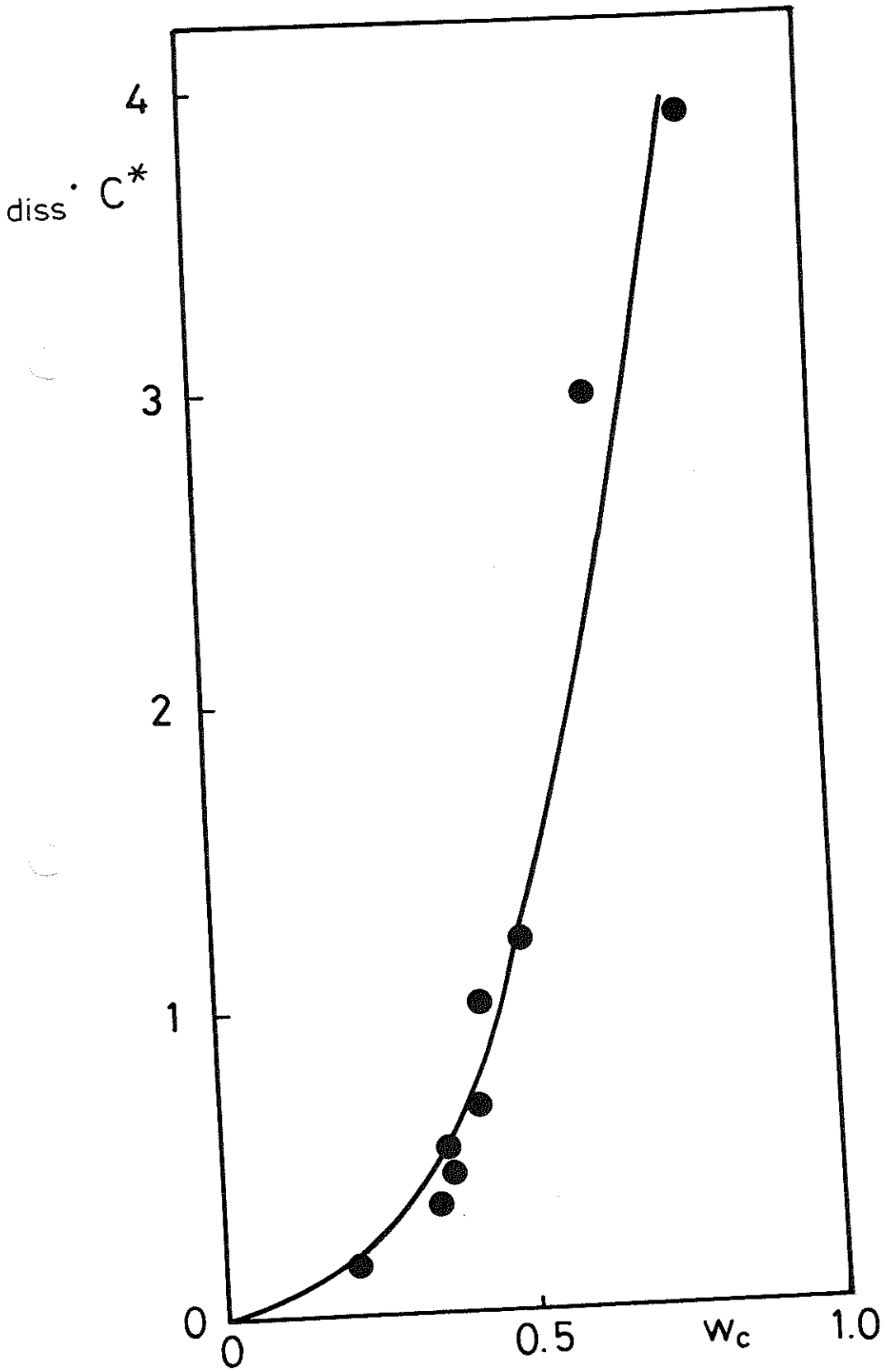

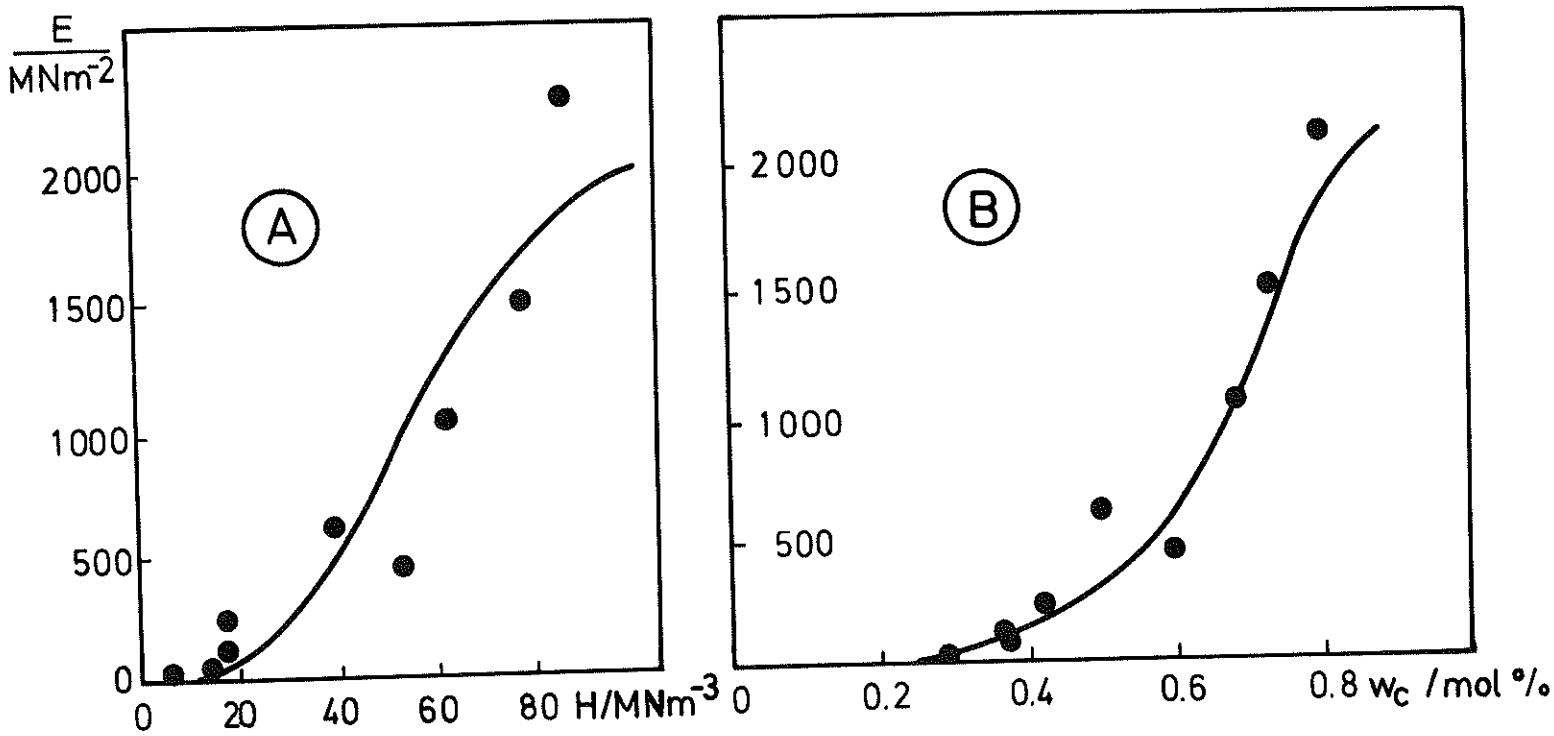
E
MNm⁻²
2000
1500
1000
500
0
A
0
20
40
60
80 H/MNm⁻³
B
2000
1500
1000
500
0
0.2
0.4
0.6
0.8 wc /mol %

Fig. 9

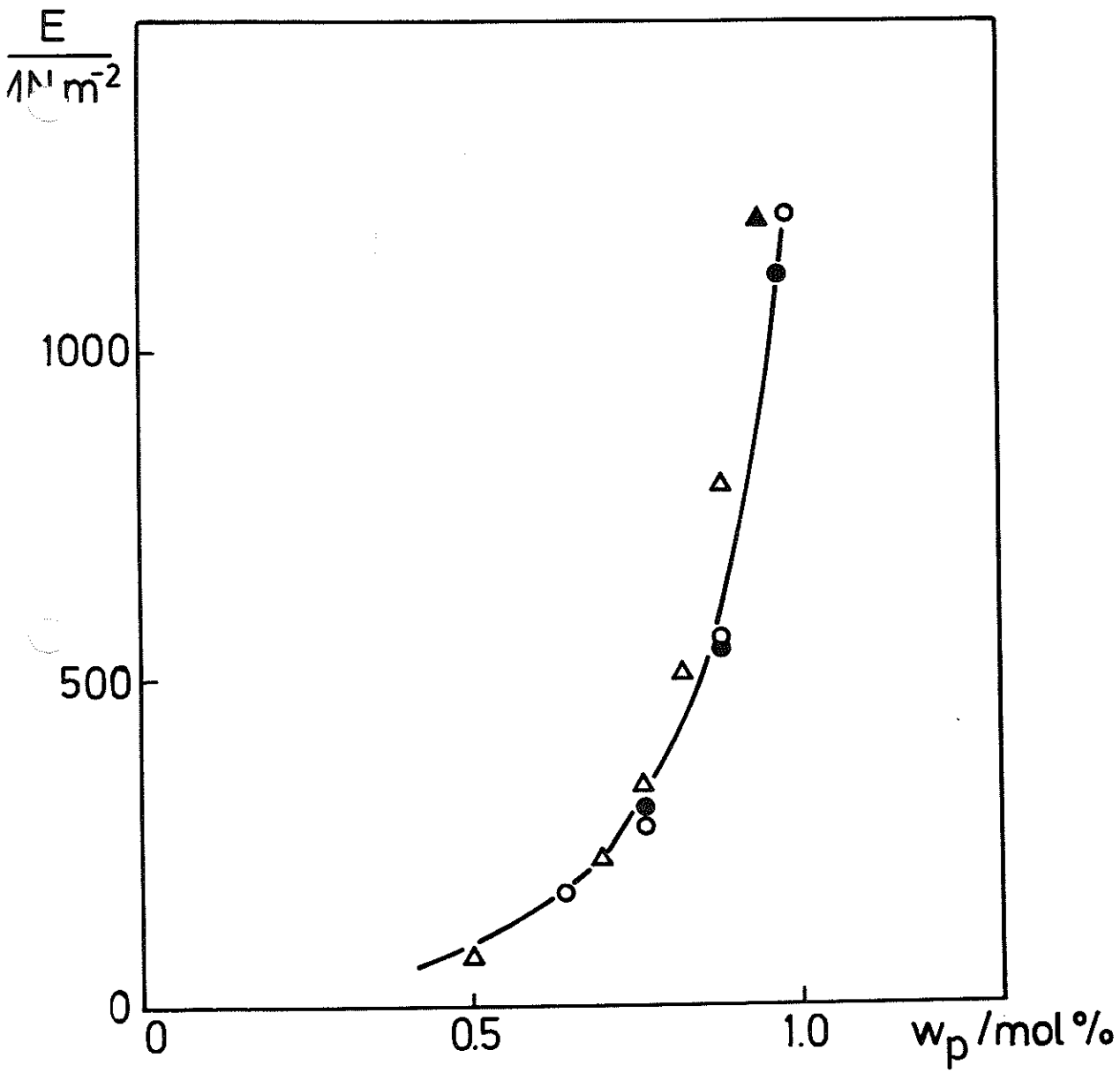

Fig. 10

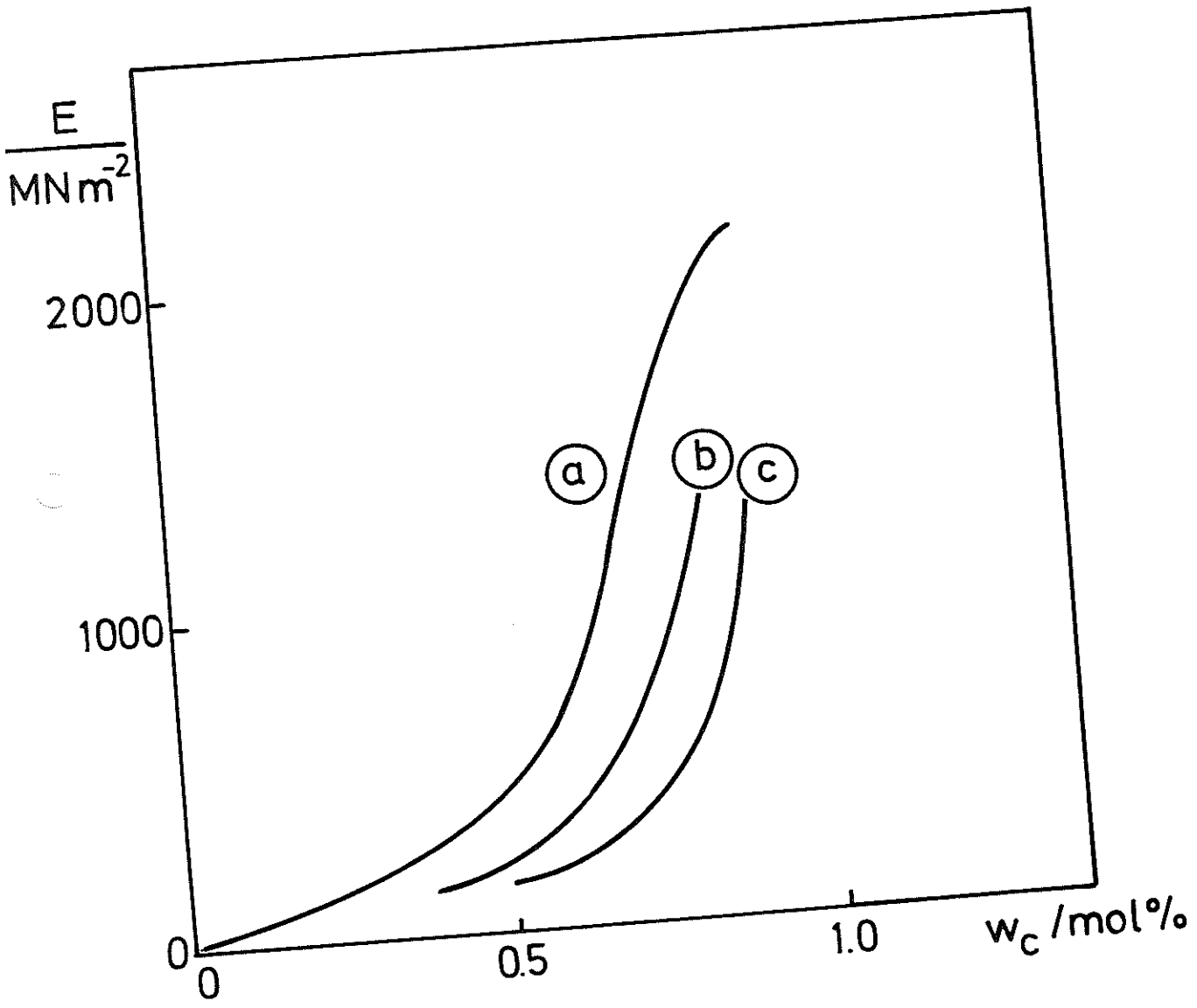

Fig 11

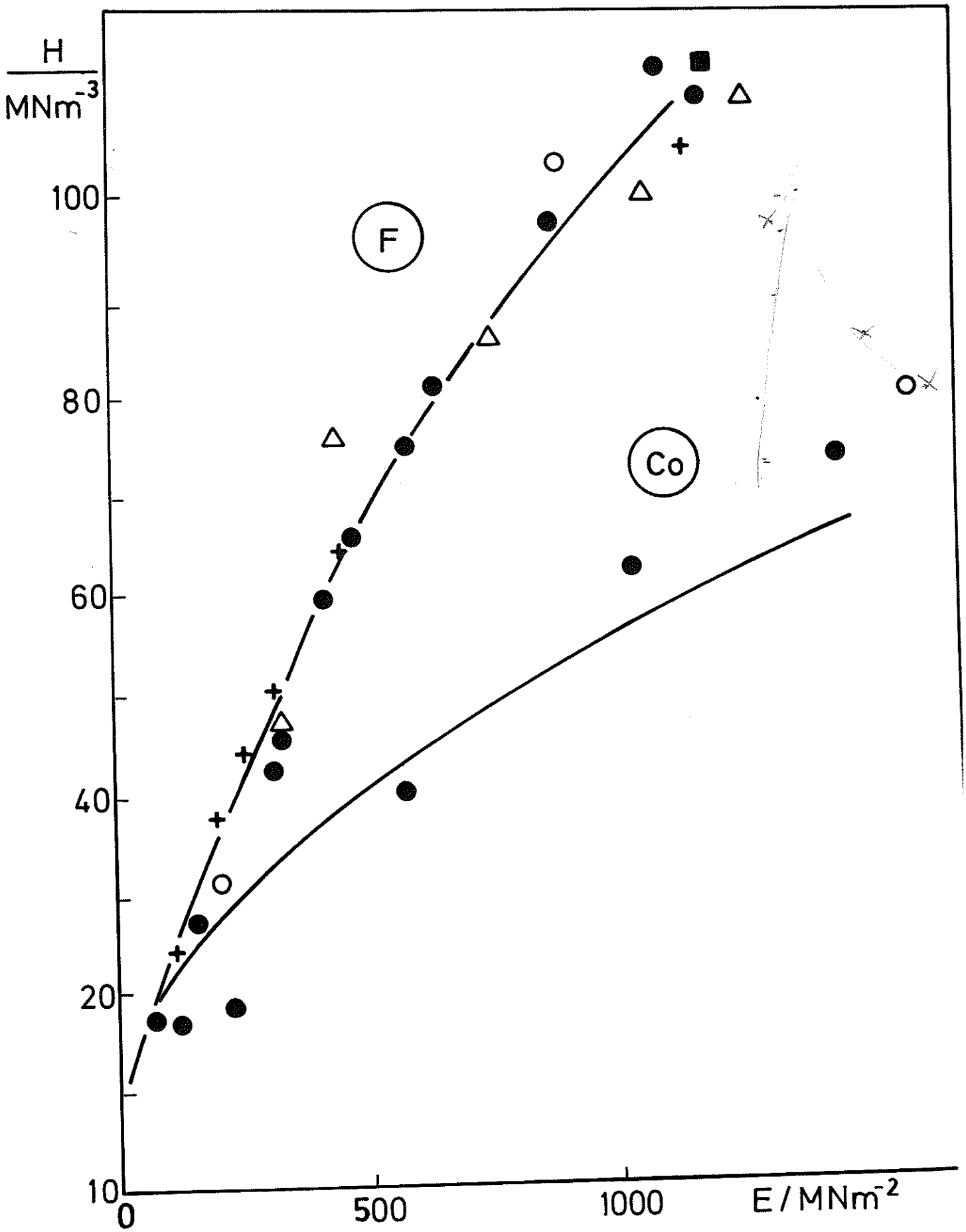

fig. 12

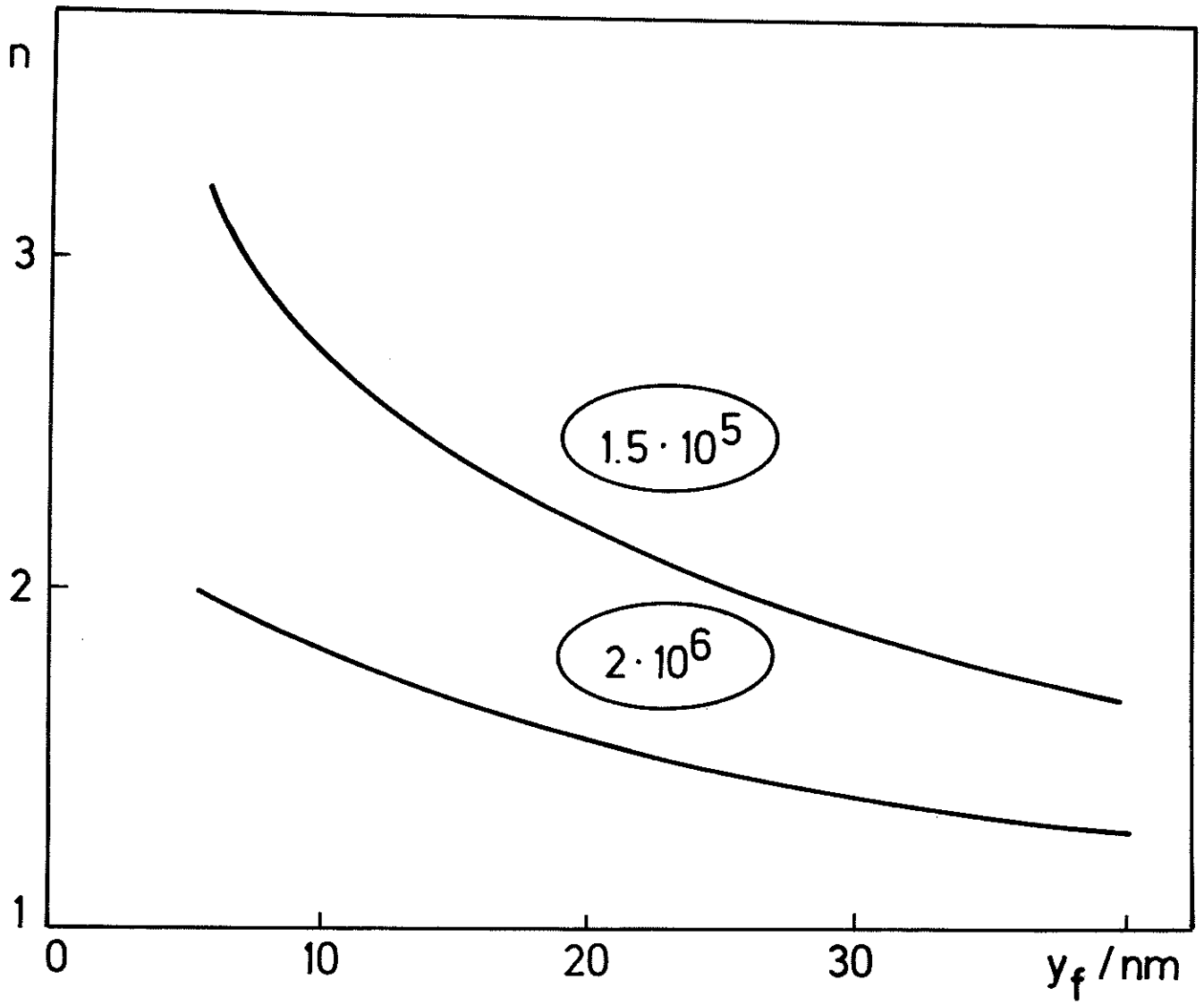

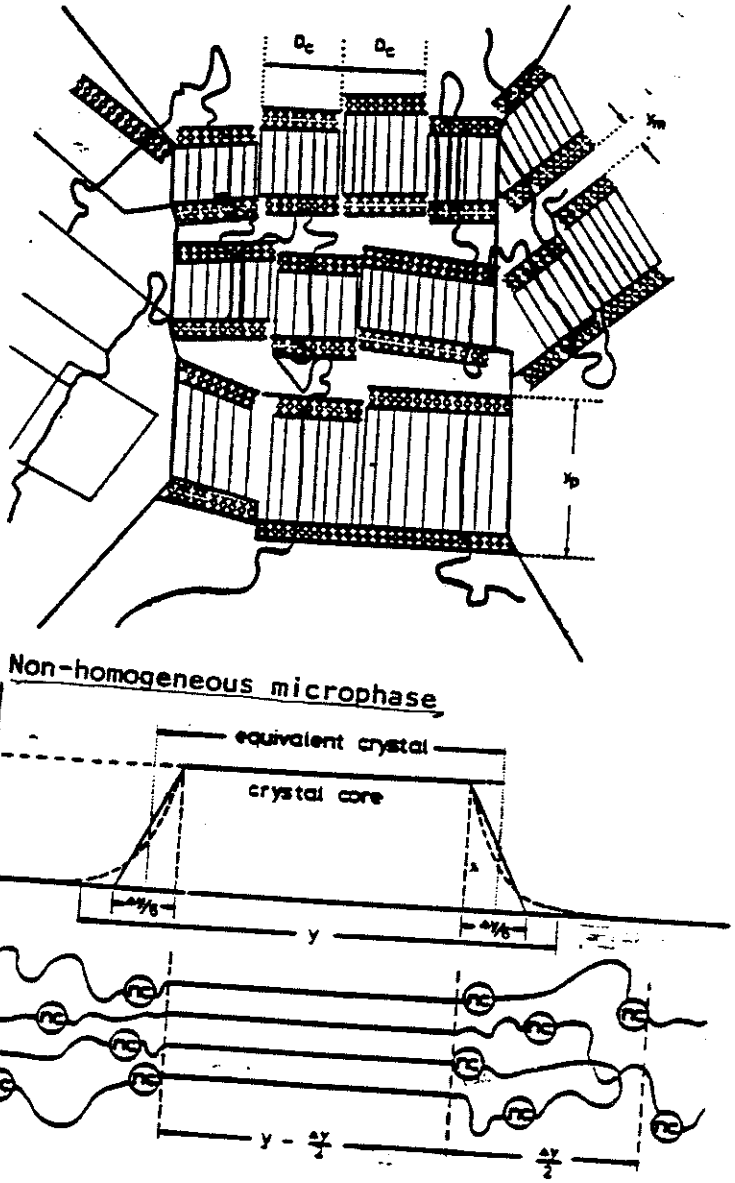
D_c
D_c
y_m
y_p
Non-homogeneous microphase
ρ
ρ_c
ρ_m
equivalent crystal
crystal core
$\Delta y/6$
y
$\Delta y/6$
nc
$y - \frac{\Delta y}{2}$
$\frac{\Delta y}{2}$

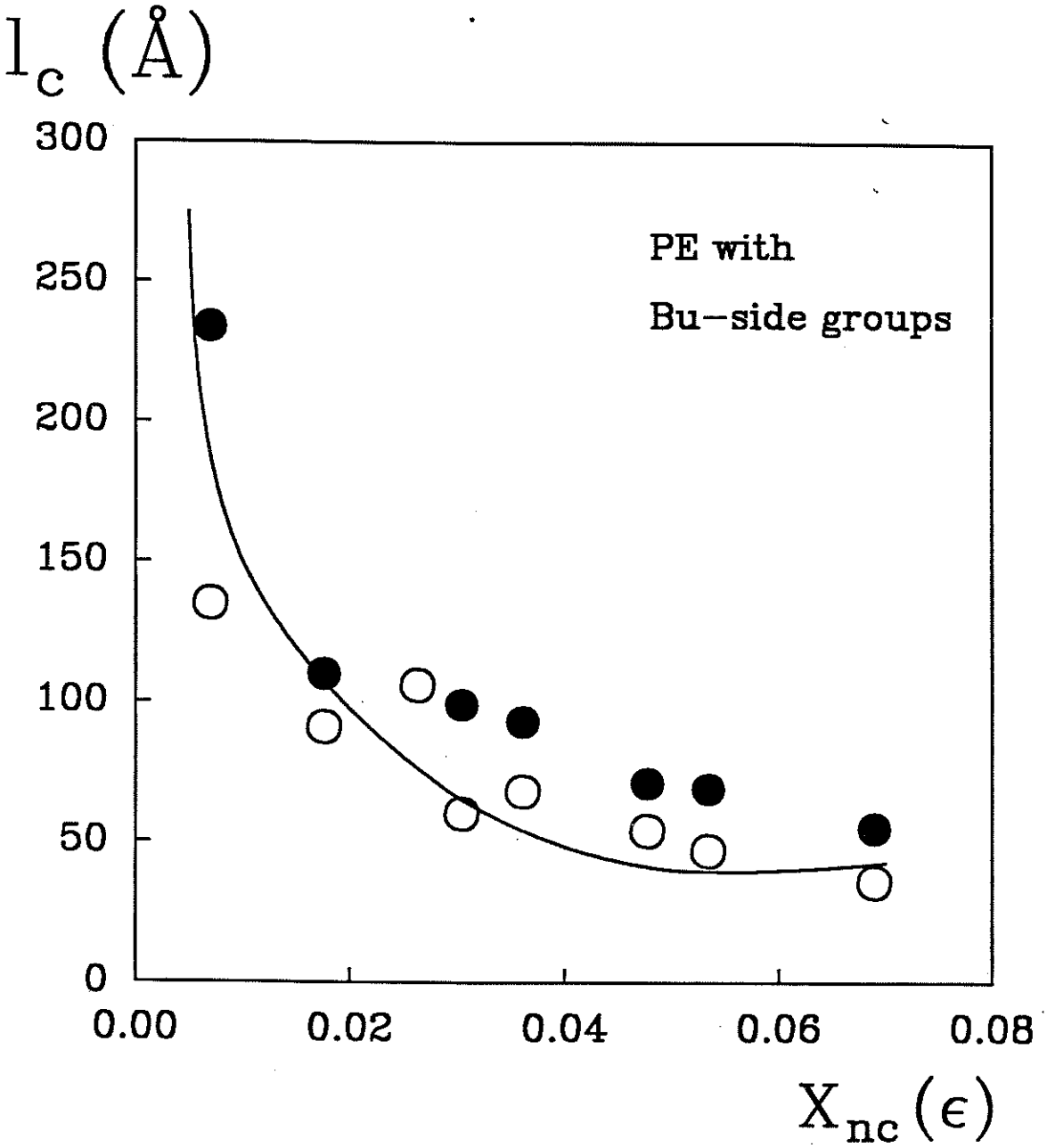
l_c (Å)
300
250
200
150
100
50
0
0.00
0.02
0.04
0.06
0.08
$X_{nc}(\epsilon)$
PE with
Bu–side groups

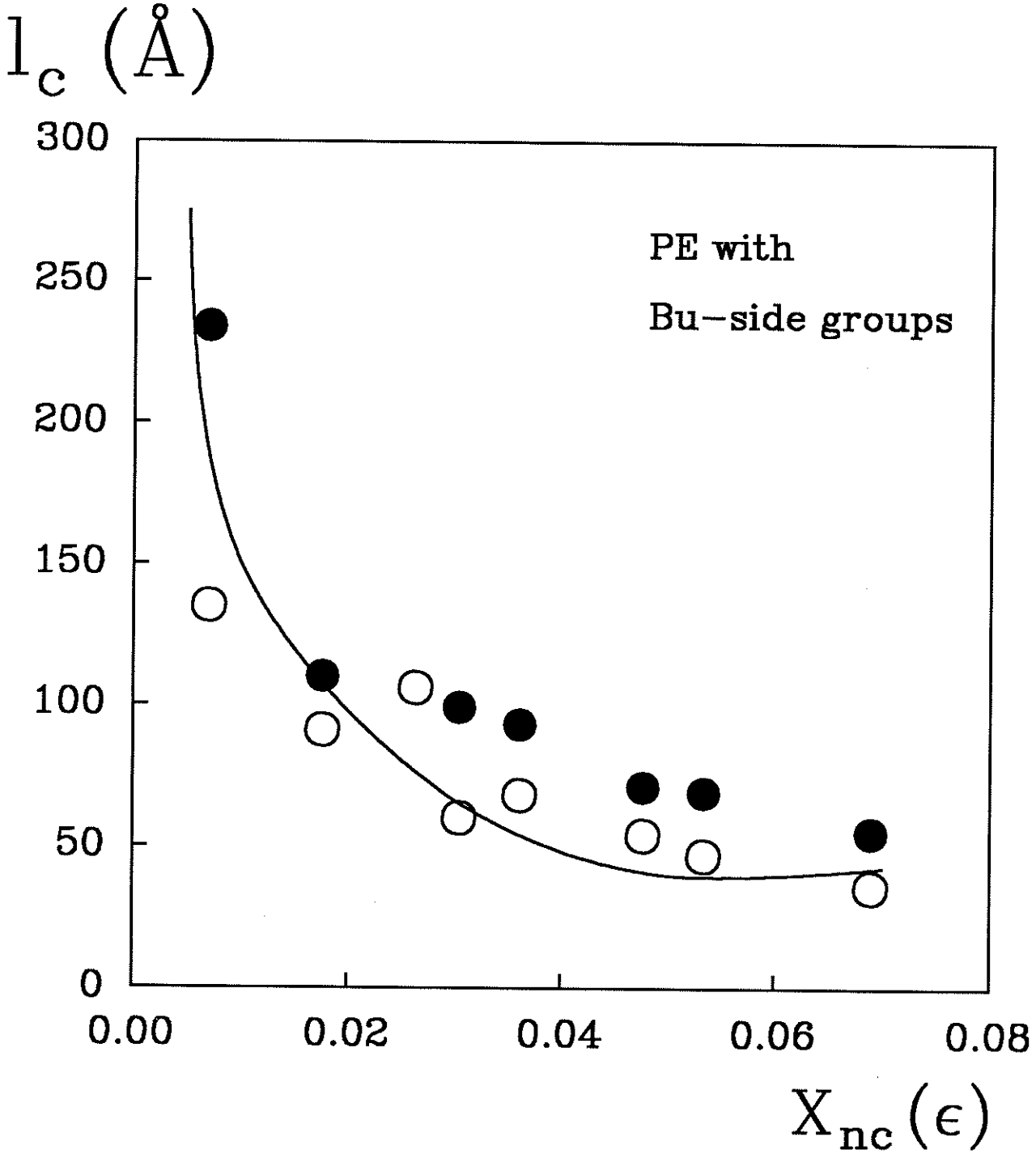
l_c (Å)
300
250
200
150
100
50
0
0.00
0.02
0.04
0.06
0.08
$X_{nc}(\epsilon)$
PE with
Bu-side groups